Energy and Buildings 133 (2016) 96–103

Contents lists available at ScienceDirect

Energy and Buildings

journal homepage: www.elsevier.com/locate/enbuild

Numerical assessment of particle dispersion and exposure risk in an underground parking lot

Yu Zhao[a,b], Jianing Zhao[b,*]

[a] Institute of Building Energy, School of Civil Engineering, Faculty of Infrastructure Engineering, Dalian University of Technology, Dalian 116024, China
[b] School of Municipal & Environmental Engineering, Harbin Institute of Technology, Harbin 150090, China

ARTICLE INFO

Article history:
Received 1 July 2016
Received in revised form
20 September 2016
Accepted 20 September 2016
Available online 21 September 2016

Keywords:
Particle dispersion
Exposure risk
Transient exhaust
Underground parking lot

ABSTRACT

The transient air flow, particle dispersion, and particle exposure risk during and after transient vehicle exhaust in an underground parking lot was investigated in the present study. The Realizable k-ε model together with particle transport theory was employed and a parking space with two cars idling and emitting exhaust and four cars at rest was established. A three-dimensional model was validated by comparing the simulated results with measured data in a residential underground parking lot of Harbin, China. Particle exposure risk during and after transient vehicle exhaust was also evaluated using the index of intake fraction. The simulation results showed that the stream of vehicle exhaust and particles dispersed from the space between two opposite cars in the upward direction during the first 30 s after vehicle exhaust was emitted. A remarkable downward dispersion of particles from the roof to the ground was observed after the vehicle stopped emitting exhaust. Intake fraction of particles increased linearly with time since exhaust and grew to approximately 1.4×10^{-3} for adult and 1.2×10^{-3} for child at 300 s after the vehicle exhaust stopped, respectively.

1. Introduction

Inhalation exposure to nanoparticles poses a significant health risk [1]. The correlation of increased disease and mortality rate from cardiovascular and respiratory diseases with particle pollution has been validated by various studies [2–4]. In most urban areas, it is believed that particles emitted from vehicles are the primary sources of nanoparticle pollution. Owing to the negative impacts on human health, prediction of vehicle particle dispersion has attracted substantial attention from the scientific community.

In China, underground parking lots are prevalent in residential areas, as ground space has become increasingly limited. In underground parking lots, vehicles park very closely; the distance between vehicles is usually no more than 0.5 m in the widthwise direction. Such parking contributes to particles congregating around the vehicles, especially in the space between the vehicles. High particle concentration attributed to congregation around the vehicles has severe damage to the health of the drivers and passengers who pass through the near wake region of the vehicles. Health is most affected during the morning rush hour when the number of vehicles with the engine running at the same time is high [5]. Furthermore, engine idling, which is quite common when a vehicle is first started, has been shown to be associated with higher exposure to nanoparticle pollution compared with moving vehicles, as the turbulent dispersion induced by the wake of a moving vehicle is absent under idling conditions [6,7]. Thermal buoyancy caused by significant temperature differences between the vehicle tailpipe and the ambient environment could also contribute to the enhancement of particle dispersion in the underground parking lot [8,9]. Combined with the high temperature difference and the enclosed environment, intensive research on characteristics of particle dispersion is essential, as this scenario is considerably different from that which would occur in an outdoor environment such as a highway or roadside.

Several methods have been employed to predict particle dispersion in different scales, such as near/far wake region of the vehicle, street canyons, neighborhoods, and cities and on a regional scale [10]. Kumar et al. reviewed the dynamics and dispersion modeling of nanoparticles from vehicles in the urban environment and indicated that flow was more turbulent and that the turbulence characteristics were unique compared with mixing features in other scales, which could result in a complex particle dispersion trend at the near wake region [11]. Since the characteristics of particle dispersion in the near wake are considerably different from the far wake and even larger scales, no series of the Gaussian theory dispersion model that could successfully assess the pollutant

* Corresponding author.
E-mail address: zhaojn@hit.edu.cn (J. Zhao).

http://dx.doi.org/10.1016/j.enbuild.2016.09.051
0378-7788/

concentrations at urban scales and far wake region of vehicle can be employed for predicting particle dispersion in the near wake. Models such as CALINE (California Line Source Dispersion Model), OSPM (Operational Street Pollution Model) and MAT (Multi-plume Aerosol dynamics and Transport) [12–16], could not be simply employed to evaluate particle dispersion in the near wake region of vehicles as the persistent recirculation and vortices in this region results in particle dispersion no longer following the Gaussian distribution model. In recent years, to overcome the disadvantage of the Gaussian dispersion model, researchers studying the development of particle dispersion in the near wake region have considered [17,18] Computational Fluid Dynamics (CFD) -based models using Reynolds Average Navier-Stokes (RANS) or Large Eddy Simulation (LES) techniques that integrate particle dynamics models. These models have recently been used for particle dispersion process in the near wake of a vehicle [6,19,20]. The dispersion of vehicle exhaust pollutants under idle conditions in congested traffic and intersections has also been studied by some researchers [21–23]. Nevertheless, most researchers have focused on predicting particle dispersion on the roadway [11] and indoors such as ventilation rooms [24,25]. The characteristics of particle dispersion under idle conditions in an enclosed environment, as is the real situation in underground parking lots, has not yet been fully understood.

Thus, the aim of this study is to analyze characteristics of particle dispersion and exposure risk at the near region of a vehicle during and after vehicle exhaust in underground parking lots, combining a Realizable k-ε model and Eulerian particle transport model. Particle size distribution was treated by nine bins based on the particle distribution measured by Gao et al. Transient air flow and particle concentration from the tailpipe during vehicle exhaust was monitored for 120 s; particle dispersion when the vehicle stopped exhausting was monitored for 300 s. Both conditions were simulated simultaneously, as this would be the realistic manner of vehicle owners in underground parking lot. Intake fraction was also considered in order to evaluate the relationship between particle pollution and human exposure.

2. Methodology

2.1. Turbulent flow model

The Realizable k-ε model developed by Shih et al. has been successfully validated to perform well for a variety of flow including jets and thermal buoyancy plumes in enclosed environments [26–28]. In this study, the Realizable k-ε model was adopted to simulate the time-dependent flow fields during and after vehicle exhaust. At the near-wall region, the Reynolds number for flow is quite low and the Realizable k-ε model that is suitable for a high Reynolds number cannot be employed. To overcome the disadvantage of Realizable k-ε model when simulating low Reynolds number flow within the near-wall region, all y^+ Wall Treatment was also employed in the study [29].

2.2. Particle transport model

To simplify the particle dynamic and transformation and to enhance simulation efficiency, this study neglected resuspension and the effect of particles on turbulent flow as particle volume fraction in the vehicle exhaust plume was very low. All particles were also assumed to be spherical in shape, and the particle density was constant during the simulation. Lastly, nucleation was not included in the study as it was already formed after 0.7 s residence time in the near wake region [11]. As the transient simulation was conducted for no more than 10 min, particle coagulation above 10 nm is too slow to substantially affect the number concentrations [11] and could also be neglected in the study. An Eulerian method that treats particles as a continuum was employed for describing particle dispersion in the study, which was consistent with our previous work [30].

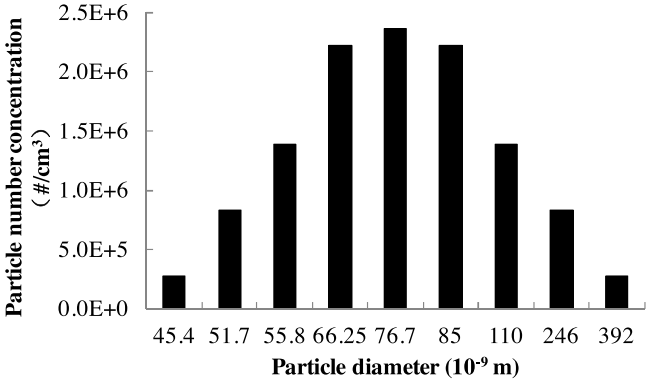

Fig. 1. Particle size distribution in the study. Particle number concentration in each bin was obtained based on sectional method in Zhao et al. [30].

Particle diameter is the key parameter for determining the particle dynamics such as deposition. In the present study, the particle size distribution and discrete methods were the same as for our previous study in our previous work [30]. The respective particle diameter and number concentration in each bin is listed in Fig. 1.

For each particle bin in Fig. 1, the governing transport equation describing the particle concentration variation is shown in Eq. (1).

$$\frac{\partial C_i}{\partial t} + \frac{\partial}{\partial x_j}[(\vec{u_j} + V_{TSi})C_i - (D_i + v_{p_i})\frac{\partial C_i}{\partial x_j}] = S_{ci} \quad (1)$$

where C_i represents particle number concentration in each particle bin (i = 1,2,...,9); x_j (j = 1,2,3) represents the three coordinates; u_j is the average air velocity components in the three directions; V_{TSi} is the terminal settling velocity of particles in each particle bin due to gravity; D_i is the Brownian diffusivity of particles in each particle bin; v_{pi} is the particle turbulent dispersion coefficient in each particle bin; and S_{ci} is the source term such as nucleation, coagulation, and condensation in each particle bin. Since these particles sink and transformations were not considered in the present study, the source term S_{ci} is 0.

The average air velocity component u_j in the three directions is computed by solving the RANS equations with the Realizable k-ε model. In addition, the velocity of particles undergoing gravitational settling V_{TSi} is mostly determined by particle size and can be calculated based on Eq. (2) [31].

$$V_{TSi} = \frac{\rho_P d_{pi}^2 g C_{ci}}{18\mu} \quad (2)$$

where ρ_p represents particle density, d_{pi} is the particle diameter in each particle bin, g is the gravitational acceleration, and C_{ci} is the Cunningham correction factor in each particle bin, which is shown in Eq. (3); μ is the kinetic viscosity of air.

$$C_{ci} = 1 + \frac{\lambda}{d_{pi}}[2.514 + 0.800\exp(-0.55\frac{d_{pi}}{\lambda})] \quad (3)$$

where λ is air mean free path. The turbulent flow is treated as ideal-gas flow in the study. The air mean free path λ can be calculated by Eq. (4).

$$\lambda = \frac{kT}{\sqrt{2}\pi d^2 p} \quad (4)$$

where k is Boltzmann's constant, 1.3807×10^{-23} J/K, T is the ambient temperature, d is the air molecule diameter, and p is the air pressure.

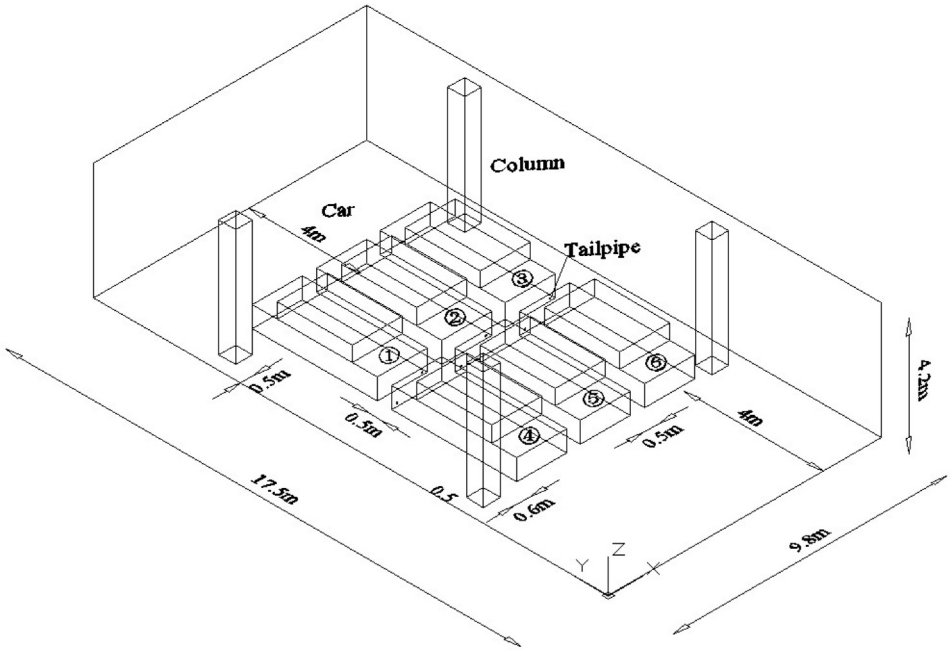

Fig. 2. Model geometry in the study. Nos. 1–6 in the figure represent car numbers in the model.

Brownian dispersion is the primary transport mechanism for particles less than 0.1 μm in size. Brownian motion is the irregular wiggling motion of an aerosol particle that is caused by random variations in the incessant bombardment of gas molecules against the particle. Transport of particles is always from an area of higher concentration to an area of lower concentration. Both processes are characterized by the particle dispersion coefficient in each particle bin D_i. The dispersion coefficient is the constant of proportionality that relates the flux of particles and the concentration gradient. This relationship is called Fick's first law of dispersion and the dispersion coefficient in each particle bin D_i can be determined by Eq. (5).

$$D_i = \frac{kTC_{ci}}{3\pi\mu d_{pi}} \tag{5}$$

Particle turbulent dispersion is common and important to consider in understanding the particle dispersion. It is relative to the fluid turbulent dispersion. The relationship between the particle turbulent dispersion coefficient v_{pi} and the air dispersion coefficient v_{ti} in each particle bin has been theoretically studied by Tchen [32]. Hinze then developed a mathematical derivation of their relation [33]. The Hinze–Tchen equation is employed for calculating the particle turbulent dispersion coefficient.

$$\frac{v_{pi}}{v_{ti}} = \left(1 + \frac{\tau_{pi}}{\tau_{ti}}\right)^{-1} \tag{6}$$

where τ_{pi} is the particle relaxation time in each bin, given by

$$\tau_{pi} = \frac{\rho_p d_{pi}^2 C_{ci}}{18\mu} \tag{7}$$

τ_{ti} is the turbulent fluctuation time, given by

$$\tau_{ti} = \sqrt{\frac{3}{2}} C_\mu^{3/4} \frac{k}{\varepsilon} \tag{8}$$

For the particle size range in the study, $\tau_{pi}/\tau_{ti} \ll 1$. Therefore, v_{pi} is equal to v_{ti}. The calculation of the air dispersion coefficient v_{ti} is performed by solving the RANS equations with the Realizable k-ε model.

3. Model procedure

3.1. Analytical model and simulation conditions

The analytical model in the study was defined as six parking spaces located in the middle of a one-storey residential underground parking lot in Harbin, China. The model geometry was 17.5 m, 9.8 m, and 4.2 m in X, Y, and Z direction, respectively. Six gasoline-powered cars with dimensions of 4.5 m (L) × 1.8 m (W) × 1.3 m (H) were placed with exhaust tailpipes opposite to one another at a distance of 0.5 m inside the parking spaces. The exhaust tailpipe exit of the studied car had a diameter of 0.05 m, was on the right side of the car, and was 0.3 m above the ground. During the particle dispersion simulation, the ambient environment was almost static. A detailed description of the model geometry can be found in Fig. 2.

Initial and boundary conditions in the model were the same as our previous research [30]. No-slip conditions were established for car surfaces, column, ceiling, and floor. The tailpipe of each car with and without engine running was defined as the velocity inlet boundary condition and the wall, respectively. According to Profession Standard of the People's Republic of China for the design of parking garage [34], air change rate in underground parking lot was usually set to 5 h^{-1}. Thus, the wall that coincided with the Y-Z plane (Fig. 2) was defined as velocity inlet. Inlet velocity through the wall was uniformly set to 0.014 m/s, which was calculated based on 5 h^{-1} air change rate in underground parking lot. Temperature and particle concentrations at this velocity inlet in the vertical direction were equal to initial condition listed in Table 1. Another opposite wall perpendicular to the X direction (Fig. 2) was defined as pressure outlet. The other two walls in the vertical direction were set to flow-slip outlet condition.

As total particles emitted from the vehicle shown in Fig. 1 was 1.18×10^{13} m^{-3}, an order of magnitude higher than ambient total particle number concentration (2.45×10^{10} m^{-3}), ambient particle concentration had little effect on the particle concentration distribution, especially at the near wake region [10]. The initial particle number concentration in each category was simplified to be equal and defined as 1/9 of the total ambient particle number concentra-

Table 1
Initial and boundary values in the simulation.

Parameters	Initial condition				Vehicle exhaust condition		
	Temperature (K)	Velocity (m/s)	Total particles (#/cm^3)	Each bin particles (#/cm^3)	Exhaust temperature (K)	Exhaust velocity (m/s)	Exhaust particles (#/cm^3)
Values	281.56	0.07 in x direction and 0 in y and z directions	2.45×10^{10}	2.72×10^{9}	303.15	1.59	1.18×10^{13}

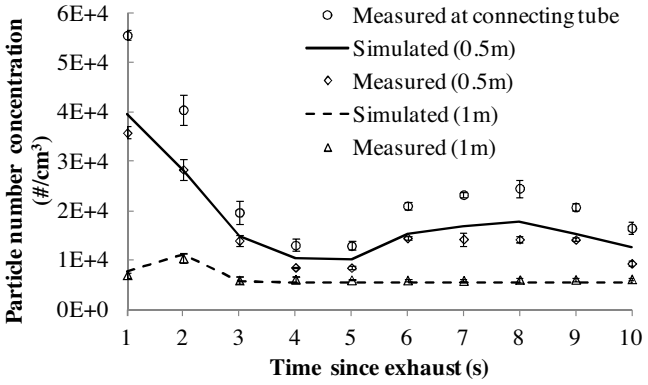

Fig. 3. Comparison of particle concentration at different locations along the centerline of tailpipe between experimental data and simulated results, Error bars represent standard deviation ($n = 3$).

tion. Initial and vehicle exhaust values in the model are given in Table 1.

According to a one-year field measurement on traffic flow in the underground parking lot [5], the maximum hourly traffic flow in one day was less than one third of the parking spaces. Thus, only two cars (Nos. 1 and 4 in Fig. 2) were set to idle running in the study. Model simulation was performed when two cars exhausted continuously and particles exhausted from the tailpipe of the car with the engine running were constant during the simulation. Particle values in each category for cars with the engine at rest were set to 0 in the study. The simulation was conducted under unsteady state conditions and lasted 120 s after vehicle engine started. Characteristics of particle dispersion and exposure level for 300 s after cars Nos. 1 and 4 stopped emitting exhaust were also evaluated in the study. The simulation model has been validated by comparing simulation results and field measurement data on transient particle dispersion along the centerline of the tailpipe behind a gasoline vehicle in a residential underground parking lot. Detailed information on model verification can be found in our previous study [30]. Fig. 3 presents the comparison of particle concentration at different locations along the centerline of tailpipe between experimental data and simulated results. The results showed that the simulation model could predict the particle dispersion well, especially at the near wake of a vehicle.

3.2. CFD methods

In order to evaluate the capability and robustness of the developed numerical model for particle dispersion, the independence tests of mesh and time step were both performed. The gradient of particle number concentration near the tailpipe was significant, and 10 s was sufficient for particles to disperse from the tailpipe to the rear of the opposite car. Thus, a point located at 0.3 m from the centerline of the tailpipe of car No. 1 and the average values of total particle number concentration among the physical model were selected for the independence tests of mesh and time step, respectively. Initial and boundary conditions for the independence

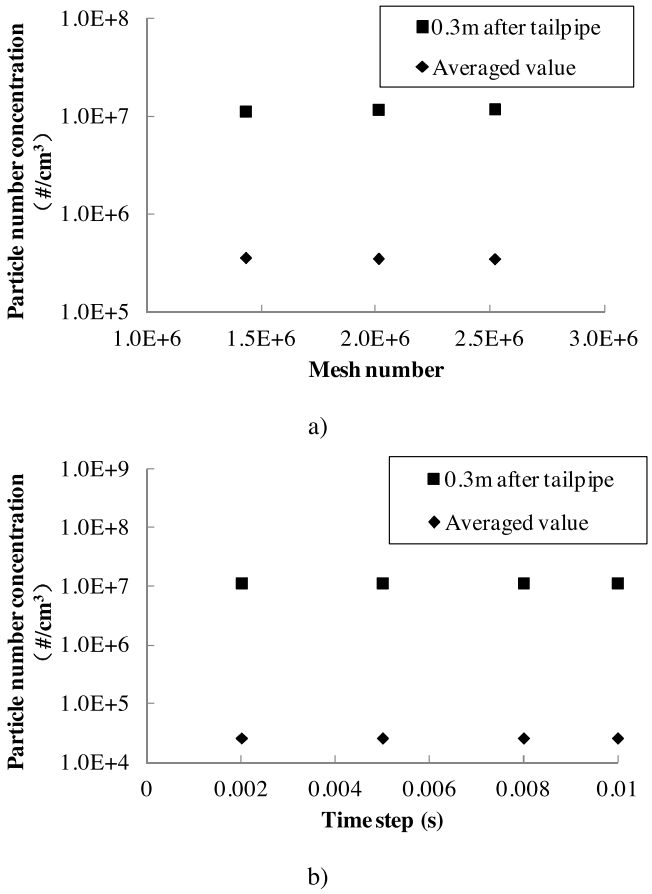

Fig. 4. The independence test of mesh and time step (a) and (b) represent mesh and time step test, respectively.

test of mesh and time step can be found in Table 1. The results in Fig. 4a reflect that the structured hexahedron mesh schemes of approximately 1,430,000 are sufficiently accurate for the particle dispersion simulation when two cars exhausted continuously in the study. The mesh was refined around the vehicle, especially near the tailpipe as shown in Fig. 5.

Fig. 4b shows the independence test of time step and particle dispersion characteristics under different time steps indicating that employing a 0.01 s time step for numerical simulation could not only ensure the calculation precision but also improve the simulation efficiency. In addition, the Courant number among each cell of the numerical model when employing 0.01 s time steps was no more than 1.

All simulations including model verification were performed using the commercial CFD software STAR CCM$^+$ [29] to solve the Realizable k-ε model for flow, pressure, and turbulence parameters. Some Passive Scalar Models with Field Functions in STAR CCM$^+$ were developed to calculate particle dispersion. The second order upwind scheme was applied to all of the convection terms in the governing equations. The SIMPLE algorithm was used for

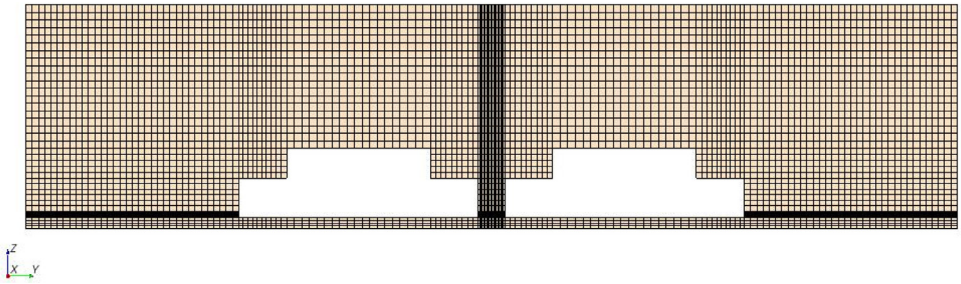

Fig. 5. Mesh constructions at the tailpipe cross section.

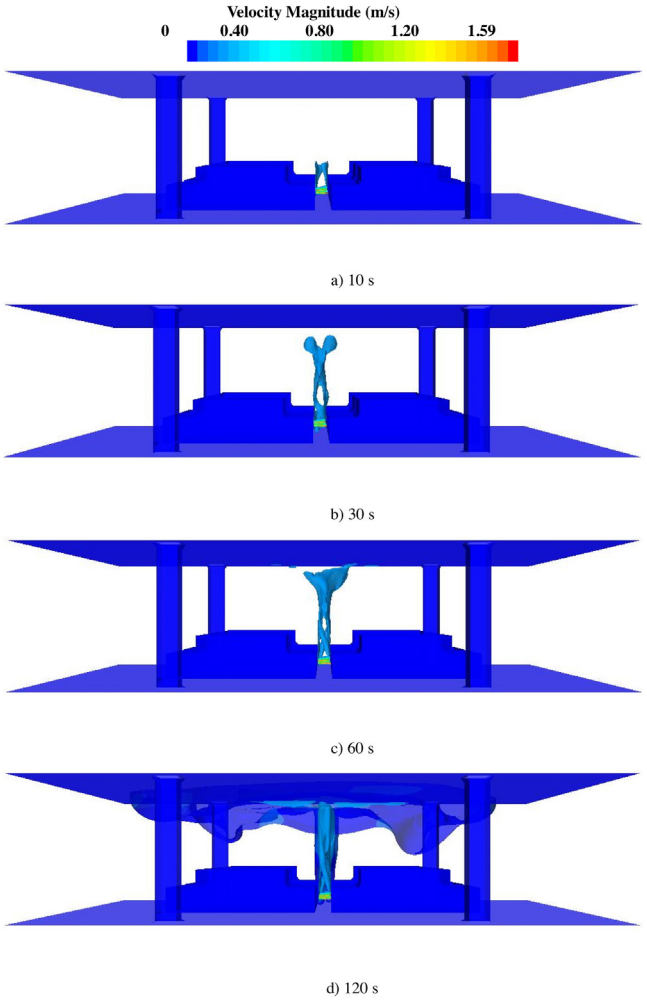

Fig. 6. Velocity magnitude at the representative time during the continuous vehicle exhaust.

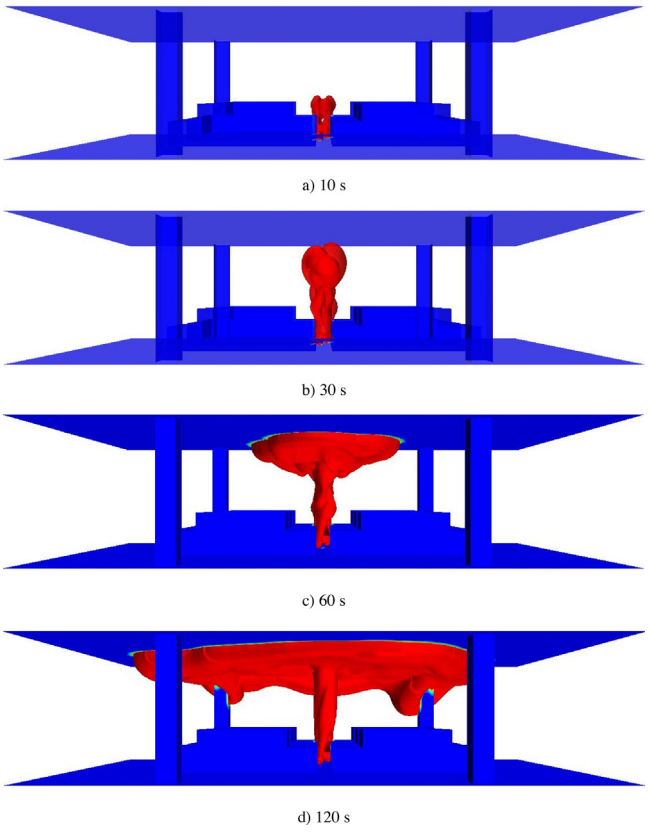

Fig. 7. Iso-value of particle number concentration 1×10^5 #/cm^3 at the representative time during the continuous vehicle exhaust.

the pressure-velocity coupling. Convergence at each time step is assumed to be obtained when all of the scaled residuals except continuity and energy reach 10^{-4} and the residuals of continuity and energy reach 10^{-6} simultaneously.

4. Results and discussion

Fig. 6 shows the velocity distribution at 10 s, 30 s, 60 s, and 120 s during the continuous vehicle exhaust. The results indicate that the jet of vehicle exhaust dispersed from the space between two opposite cars in the upward direction during the first 30 s after the vehicle exhausted. The block and squeeze from the narrow space of the opposite cars and thermal buoyancy force induced by the temperature difference between the vehicle exhaust and the ambient environment in the underground parking lot could attribute to the obvious upward motion in less than 30 s during continuous exhaust. During 30 s and 120 s, due to the obstruction of the roof, the exhaust jet gradually accumulated and dispersed near the roof in a horizontal direction. The characteristic of velocity distribution in the underground parking lot could influence the particle dispersion and accumulation, particularly near the tailpipe and roof.

In addition, the iso-value of particle concentration 1×10^5 #/cm^3, which is nearly five times higher than in the ambient environment (2.45×10^4 #/cm^3) and could reflect characteristics of particle distribution, was employed for analyzing transient particle dispersion. Fig. 7 presents the iso-value of particle concentration 1×10^5 #/cm^3 at 10 s, 30 s, 60 s, and 120 s after the vehicle exhausted. Similar to velocity distribution, particles exhausted from idle cars dispersed obviously from the narrow space between the opposite cars to the roof in less than 30 s. The results could demonstrate that the motion of vehicle exhaust particles was in accordance with the vehicle exhaust jet.

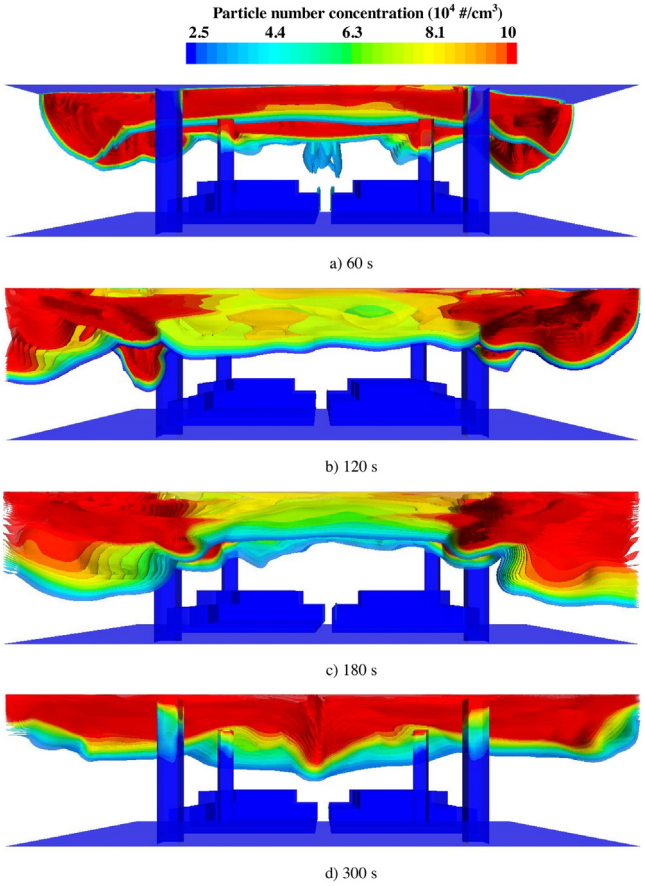

Fig. 8. Distribution of particle number concentration at the representative time when vehicle stopped exhausting.

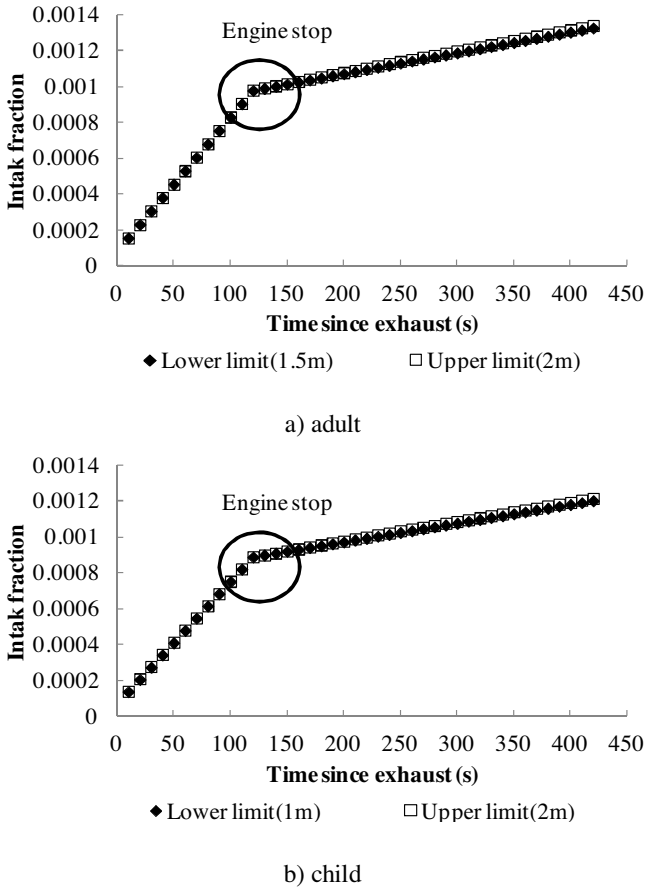

Fig. 9. Intake fraction of particles for adult and child.

As exhaust time increased, particles accumulated near the roof and horizontal dispersion along the roof was significant after 60 s. When the vehicle exhausted for 120 s, particle concentration at the area higher than 2.5 m above the ground in the model was no less than 1×10^5 #/cm^3. This observation could reflect that the particle diffusion velocity in the downward direction was quite fast during 60 s and 120 s after the vehicle exhausted. The accumulated particles might have severe impact on the health of occupants around the parking space in the underground parking lot.

Fig. 8 shows characteristics of particle dispersion at 60 s, 120 s, 180 s, and 300 s when the vehicle engine stopped after 120 s of continuous exhaust. A remarkable downward dispersion of the particles from the roof to the ground was observed through numerical simulation. Particle dispersion from the area directly over the particle source (cars Nos. 1 and 4) to the region over the other cars was easily observable. It could be attributed to the gradient of particle concentration in both the vertical and horizontal directions, induced by the accumulation of particles near the roof over the exhaust source during continuous exhaust (Fig. 6c and d). After the vehicle stopped exhausting, the particle number concentration at the same height appeared to fluctuate until 300 s. The greater the height, the more significant the fluctuation was as shown in Fig. 7. Meanwhile, particle number concentration decreased with the increase of time and a hierarchical distribution of particles was obtained at 300 s after the vehicle stopped exhausting. The gradient of particles from the roof to the ground would also affect the human exposure to particle pollution in an underground parking lot.

As Figs. 7 and 8 shows, particle dispersion under transient exhaust conditions was significantly different from what would be observed in open spaces and other indoor environments. It is necessary to identify the particle exposure level in the underground parking lot during and after transient exhaust conditions. The particle exposure was evaluated by intake fraction (IF) [35], which could be expressed as the ratio of the particles inhaled by a person across the interface to the particles emitted from the source. The intake fraction (IF) was calculated by Eq. (9).

$$IF = \frac{\int_{t_1}^{t_2} C(t)IR(t)dt}{M} \tag{9}$$

where $C(t)$ represents transient particle concentration, $IR(t)$ is the respiratory rate, and M refers to episodic emission quantity of vehicle exhaust particles during a rapid period from time t_1 to time t_2.

For a time-dependent episodic emission, particle contaminant is released from the source into the underground parking lot at some rate $E(t)$, such that

$$M = \int_{t_1}^{t_2} E(t)dt \tag{10}$$

Fig. 9 presents the averaged intake fraction of particles at the respiratory region for a single adult (age ≥16) or child (age 0–16) during and after the transient exhaust conditions. The respiratory region for adult and child along the vertical direction is 1.5–2 m and 1–2 m, respectively. Based on the recommendation by the U.S. Environmental Protection Agency [36], the respiratory rate differs for adult and child, and is 2.04×10^{-4} m^3/(s person) and 1.85×10^{-4} m^3/(s person), respectively.

Table 2
Comparison of intake fraction for particles indoors and outdoors.

Literature	Location	Air change rate (h^{-1})	Particle source	Method	IF (per million)
This study	Indoor (parking lot)	5	Vehicle emission	CFD model	1334 at 420 s (0.02–0.4 μm)
He et al. [38]	Indoor (office)	0.37–3.47	Respiratory droplets	CFD model	20–1380 (0.8 μm)
Gao et al. [39]	Indoor (office)	3.81	Coughing particles	CFD model	4634 at 7200 s (0.7 μm)
Du et al. [40]	Outdoor (Beijing)	–	Vehicle emission	Personal exposure data	153 ($PM_{2.5}$)[a]
Marshall et al. [41]	Outdoor (US urban areas)	–	Vehicle emission	One-compartment Empirical National-scale Air Toxics	5.7–54[a]

[a] The intake fraction here was the individual value multiplied by population number.

A significant inflection point at 120 s was observed due to the vehicle engine stalling. IF increased linearly with the increase in time from exhaust during and after transient exhaust conditions. However, the growth rate of IF during the transient exhaust period was larger than the period after 120 s of continuous exhaust. This observation could be contributed to a high particle exposure level at the respiratory region during continuous exhaust, especially at the region directly above the space between two opposite cars (Nos. 1 and 4). As time increased to 300 s from exhaust, the intake fraction of particles for a single adult and child was almost 1.4×10^{-3} and 1.2×10^{-3}, respectively.

Lai et al. pointed out that IF ranged enormously, from 10^{-12} to 10^{-1} [37]. The most significant variable influencing the magnitude of the IF was whether the emission occurred indoors (or in a vehicle) or outdoors. Thus, a series of studies on particle exposure analysis indoors and outdoors was compared and listed in Table 2 [38–41]. Since air change rate of indoor environment was a key factor influencing IF, the ranges of air change rate among this study and other indoor studies [38,39] were also listed in Table 2 for comparison.

In accordance with Lai et al., intake fraction of particles in the residential underground parking lot in this study was at least an order of magnitude higher than outdoors, including in Beijing and US urban areas. Particle exposure risk in the residential underground parking lot was much higher than in the outdoor environment. It could also be found in Table 2 that air change rate in this study was nearly 13.5 times higher than the minimum in He et al. [38]. Ratio of IF value between this study and the minimum in He et al. [38] was 66.7. The results once again demonstrated that air change rate at indoor environments had great impact on IF values. However, Gao et al. [39] found that the exposure level of episodic coughing particle emission at 7200 s was even 3 times higher than observed in this study, although air change rate in this study was 1.3 times higher than the value in Gao et al. [39]. In less than 15 s, the exposure risk of coughing emission reached the same level (1300 per million), in a much shorter time compared with this study. This could be attributed to fewer obscure parts in an office and a short distance between the coughing person and healthy person. In addition, the particle emission source was close to the respiratory region in [39]. Particles could rapidly disperse to the region around the healthy person without obstruction, which was a different scenario than that of our study.

5. Conclusion

The present study focused on particle dispersion and exposure risk in a residential underground parking lot during a 120 s continuous vehicle exhaust and a 300 s transient dispersion after the vehicle exhaust stopped. The conclusions are as follows:

1. During the 120 s transient exhaust period, the exhaust jet and particles dispersed from the space between two opposite cars in the upward direction during the first 30 s after the vehicle emitted exhaust. Owing to the obstruction of the roof, the exhaust jet and particles gradually accumulated and dispersed near the roof in a horizontal direction. Particle concentration at the area higher than 2.5 m above the ground in the model was no less than 1×10^5 #/cm^3.
2. When the two cars stopped emitting exhaust, a remarkable downward dispersion of particles from the roof to the ground was observed. Particle dispersion from the area directly over the particle source (cars Nos. 1 and 4) to the region over the other cars was easily observable. Particle number concentration at the same height appeared to fluctuate over 300 s and the fluctuation range increased with the height in the parking lot. Particle number concentration degenerated with the increase of time and a hierarchical distribution of particles was obtained at 300 s.
3. Intake fraction (IF) is a useful tool to link pollutant emissions from a particle source and population exposure. IF increased linearly with time since exhaust during and after transient exhaust conditions. However, the growth rate of IF during the transient exhaust period was larger than the period when the vehicle engine stopped. As time increased to 300 s since exhaust, intake fraction of particles for a single adult and child in the underground parking lot was almost 1.4×10^{-3} and 1.2×10^{-3}, respectively, which was at least an order of magnitude higher than would be observed from a vehicle emission particle source outdoors.

Acknowledgements

This work was supported by “the Fundamental Research Funds for the Central Universities” in China (grant number: 1103-852041). The authors wish to acknowledge Yan Wang and Kai Zhu at the School of Municipal and Environmental Engineering, Harbin Institute of Technology in China for their assistances with model validation, the boundary and initial conditions measurement in the simulation.

References

[1] F. Dominici, R.D. Peng, M.L. Bell, L. Pham, A. McDermott, S.L. Zeger, J.M. Samet, Fine particulate air pollution and hospital admission for cardiovascular and respiratory diseases, J. Am. Med. Assoc. 295 (2006) 1127–1134.
[2] S.V. Klot, G. Wölke, T. Tuch, J. Heinrich, D.W. Dockery, J. Schwartz, W.G. Kreyling, H.E. Wichmann, A. Peters, Increased asthma medication use in association with ambient fine and ultrafine particles, Eur. Respir. J. 20 (2002) 691–702.
[3] T. Nicolai, D. Carr, S.K. Weiland, H. Duhme, O.V. Ehrenstein, C. Wagner, E.V. Mutius, Urban traffic and pollutant exposure related to respiratory outcomes and atopy in a large sample of children, Eur. Respir. J. 21 (2003) 956–963.

[4] A. Peters, S.V. Klot, M. Heier, I. Trentinaglia, A. Hörmann, W.H. Erich, H. Löwel, Exposure to traffic and the onset of myocardial infarction, N. Engl. J. Med. 351 (2004) 1721–1730.
[5] Y. Zhao, J.N. Zhao, Field study on PM1 air pollution in a residential underground parking lot, Proceedings of 8th International Symposium on Heating, Ventilation and Air Conditioning 1 (2013) 281–288.
[6] P.Z. Jiang, D.O. Lignell, K.E. Killy, J.S. Lighty, A.F. Sarofim, C.J. Montgomery, Simulation of the evolution of particle size distributions in a vehicle exhaust plume with unconfined dilution by ambient air, J. Air Waste Manage. Assoc. 55 (2005) 437–445.
[7] Y.H. Liu, Z. He, T.L. Chan, Three-dimensional simulation of exhaust particle dispersion and concentration fields in the near-wake area of the studied ground vehicle, Aerosol Sci. Technol. 45 (2011) 1019–1030.
[8] C.A. Alves, D.J. Lopes, A.I. Calvo, M. Evtyugina, S. Rocha, T. Nunes, Emissions from light-duty diesel and gasoline in-use vehicles measured on chassis dynamometer test cycles, Aerosol Air Qual. Res. 15 (2014) 99–116.
[9] J.D. Gao, C.L. Song, T.C. Zhang, J.R. Fan, J.H. Gao, S.X. Liu, Size distributions of exhaust particulates from a passenger car with gasoline engine, J. Combust. Sci. Technol. 13 (2007) 248–252.
[10] R.E. Britter, S.R. Hanna, Flow and dispersion in urban areas, Annu. Rev. Fluid Mech. 35 (2003) 469–496.
[11] P. Kumar, M. Ketzel, S. Vardoulakis, L. Pirjola, R. Britter, Dynamics and dispersion modelling of nanoparticles from road traffic in the urban atmospheric environment—a review, J. Aerosol Sci. 42 (2011) 580–603.
[12] P.E. Benson, A review of the development and application of the CALINE3 and 4 models, Atmos. Environ. 26 (1992) 379–390.
[13] R. Berkowicz, Operational street pollution model—a parameterized street pollution, Environ. Monit. Assess. 65 (2000) 323–331.
[14] M. Ketzel, R. Berkowicz, Multi-plume aerosol dynamics and transport model for urban scale particle pollution, Atmos. Environ. 39 (2005) 3407–3420.
[15] M. Carpentieri, P. Kumar, A. Robins, An overview of experimental results and dispersion modelling of nanoparticles in the wake of moving vehicles, Environ. Pollut. 159 (2011) 685–693.
[16] P. Sharma, M. Khare, Modelling of vehicular exhausts—a review, Transp. Res.: D 6 (2001) 179–198.
[17] Z.E. Hider, S. Hibberd, C.J. Baker, Modelling particulate dispersion in the wake of a vehicle, J. Wind Eng. Ind. Aerodyn. (1997) 733–744, 67&68.
[18] B. Bessagnet, R. Rosset, Fractal modelling of carbonaceous aerosols-application to car exhaust plumes, Atmos. Environ. 35 (2001) 4751–4762.
[19] D.H. Kim, M. Gautam, D. Gera, On the prediction of concentration variations in a dispersing heavy-duty truck exhaust plume using κ-ε turbulent closure, Atmos. Environ. 35 (2001) 5267–5275.
[20] Z.Q. Yin, J.Z. Lin, K. Zhou, T.L. Chan, Numerical simulation of the formation of pollutant nanoparticles in the exhaust twin-jet plume of a moving car, Int. J. Nonlinear Sci. Numer. Simul. 8 (2007) 535–544.
[21] Z. Ning, C.S. Cheung, Y. Liu, M.A. Liu, W.T. Hung, Experimental and numerical study of the dispersion of motor vehicle pollutants under idle condition, Atmos. Environ. 39 (2005) 7880–7893.
[22] J.S. Kinsey, D.C. Williams, Y. Dong, R. Logan, Characterization of fine particle and gaseous emissions during school bus idling, Environ. Sci. Technol. 41 (2007) 4972–4979.
[23] A. McNabola, B.M. Broderick, L.W. Gill, The impacts of inter-vehicle spacing on in-vehicle air pollution concentrations in idling urban traffic conditions, Transp. Res.: D 14 (2009) 567–575.
[24] H.M. Kao, T.J. Chang, Y.F. Hsieh, C.H. Wang, C.I. Hsieh, Comparison of airflow and particulate matter transport in multi-room buildings for different natural ventilation patterns, Energy Build. 41 (2009) 966–974.
[25] T. Lim, J. Cho, B.S. Kim, The predictions of infection risk of indoor airborne transmission of diseases in high-rise hospitals: tracer gas simulation, Energy Build. 42 (2010) 1172–1181.
[26] T.H. Shih, W.W. Liou, A. Shabbir, Z.G. Yang, J. Zhu, A new κ-ε eddy viscosity model for high Reynolds number turbulent flows, Comput. Fluids 24 (1995) 227–238.
[27] E. Rusly, L. Aye, W.W.S. Charters, A. Ooi, CFD analysis of ejector in a combined ejector cooling system, Int. J. Refrig. 28 (2005) 1092–1101.
[28] Z.Q. Zhai, Z. Zhang, W. Zhang, Q.Y. Chen, Evaluation of various turbulence models in predicting airflow and turbulence in enclosed environments by CFD: part 1—summary of prevalent turbulence models, HVAC&R Res. 13 (2007) 853–870.
[29] CD-adapco, USER GUIDE STAR-CCM+ Version 8.02, CD-adapco, New York, 2013.
[30] Y. Zhao, S. Kato, J.N. Zhao, Numerical analysis of particle dispersion characteristics at the near region of vehicles in a residential underground parking lot, J. Dispers. Sci. Technol. 36 (2015) 1327–1338.
[31] W.C. Hinds, Aerosol Technology, John Wiley and Sons, New York, 1982.
[32] C.M. Tchen, Mean Value and Correlation Problems Connected with the Motion of Small Particles Suspended in a Turbulent Fluid, Delft University of Technology, Netherland, 1974.
[33] J.O. Hinze, Turbulence, 2nd edn., McGraw-Hill, New York, 1975.
[34] Ministry of Housing and Urban-Rural Construction of the People's Republic of China (MOHURD), Code for design of parking garage building (2015).
[35] W.W. Nazaroff, Inhalation intake fraction of pollutants from episodic indoor emissions, Build. Environ. 43 (2008) 269–277.
[36] U.S. Environmental Protection Agency, Exposure Factors Handbook, 2011 edn., National Center for Environmental Assessment, Washington, DC, 2011.
[37] A.C.K. Lai, T.L. Thatcher, W.W. Nazaroff, Inhalation transfer factors for air pollution health risk assessment, J. Air Waste Manage. Assoc. 50 (2000) 1688–1699.
[38] Q. He, J. Niu, N. Gao, T. Zhu, J. Wu, CFD study of exhaled droplet transmission between occupants under different ventilation strategies in a typical office room, Build. Environ. 46 (2011) 397–408.
[39] J. Gao, C. Cao, Z. Luo, X. Zhang, Inhalation exposure to particulate matter in rooms with underfloor air distribution, Indoor Built Environ. 23 (2014) 236–245.
[40] X. Du, Y. Wu, L. Fu, S. Wang, S. Zhang, J. Hao, Intake fraction of $PM_{2.5}$ and NO_X from vehicle emissions in Beijing based on personal exposure data, Atmos. Environ. 57 (2012) 233–243.
[41] J.D. Marshall, S.K. Teoh, W.W. Nazaroff, Intake fraction of nonreactive vehicle emissions in US urban areas, Atmos. Environ. 39 (2005) 1363–1371.